

## High accuracy $^{235}\text{U}(n,f)$ data in the resonance energy region

C. Paradelo<sup>1,2,a</sup>, I. Duran<sup>2</sup>, L. Tassan-Got<sup>3</sup>, L. Audouin<sup>3</sup>, B. Berthier<sup>3</sup>, S. Isaev<sup>3</sup>, C. Le Naour<sup>3</sup>, C. Stephan<sup>3</sup>, D. Tarrío<sup>2,17</sup>, U. Abbondanno<sup>4</sup>, G. Aerts<sup>5</sup>, H. Álvarez-Pol<sup>2</sup>, F. Álvarez-Velarde<sup>6</sup>, S. Andriamonje<sup>5</sup>, J. Andrzejewski<sup>7</sup>, G. Badurek<sup>8</sup>, P. Baumann<sup>9</sup>, F. Becvar<sup>10</sup>, E. Berthoumieu<sup>5</sup>, F. Calviño<sup>11</sup>, M. Calviani<sup>12</sup>, D. Cano-Ott<sup>6</sup>, R. Capote<sup>13</sup>, C. Carrapiço<sup>14</sup>, P. Cennini<sup>12</sup>, V. Chepel<sup>15</sup>, E. Chiaveri<sup>12</sup>, N. Colonna<sup>16</sup>, G. Cortes<sup>11</sup>, A. Couture<sup>17</sup>, J. Cox<sup>17</sup>, M. Dahlfors<sup>12</sup>, S. David<sup>3</sup>, I. Dillmann<sup>18</sup>, C. Domingo-Pardo<sup>19</sup>, W. Dridi<sup>5</sup>, C. Eleftheriadis<sup>20</sup>, M. Embid-Segura<sup>10</sup>, L. Ferrant<sup>3</sup>, A. Ferrari<sup>12</sup>, R. Ferreira-Marques<sup>15</sup>, K. Fujii<sup>21</sup>, W. Furman<sup>22</sup>, I.F. Gonçalves<sup>14</sup>, E. Gonzalez-Romero<sup>6</sup>, A. Goverdovski<sup>23</sup>, F. Gramegna<sup>24</sup>, C. Guerrero<sup>12,13</sup>, F. Gunsing<sup>5</sup>, R. Haight<sup>25</sup>, M. Heil<sup>18</sup>, M. Igashira<sup>26</sup>, E. Jericha<sup>8</sup>, Y. Kadi<sup>12</sup>, F. Kaeppler<sup>18</sup>, D. Karadimos<sup>27</sup>, M. Kerveno<sup>8</sup>, V. Ketlerov<sup>23</sup>, P. Koehler<sup>25</sup>, V. Konovalov<sup>22</sup>, M. Krlicka<sup>10</sup>, C. Lampoudis<sup>20</sup>, C. Lederer<sup>8</sup>, H. Leeb<sup>8</sup>, A. Lindote<sup>15</sup>, S. Lukic<sup>9</sup>, J. Marganec<sup>7</sup>, T. Martinez<sup>6</sup>, S. Marrone<sup>16</sup>, C. Massimi<sup>28</sup>, P. Mastinu<sup>24</sup>, A. Mengoni<sup>12,2</sup>, P.M. Milazzo<sup>21</sup>, C. Moreau<sup>21</sup>, M. Mosconi<sup>18</sup>, S. J. Pancin<sup>5</sup>, A. Pavlik<sup>42</sup>, P. Pavlopoulos<sup>28</sup>, L. Perrot<sup>5</sup>, R. Plag<sup>18</sup>, A. Plompen<sup>1</sup>, A. Plukis<sup>5</sup>, A. Poch<sup>11</sup>, C. Pretel<sup>11</sup>, J. Praena<sup>24</sup>, J. Quesada<sup>13</sup>, T. Rauscher<sup>30</sup>, R. Reifarth<sup>25</sup>, C. Rubbia<sup>12</sup>, G. Rudolf<sup>9</sup>, P. Rullhusen<sup>1</sup>, J. Salgado<sup>14</sup>, C. Santos<sup>14</sup>, L. Sarchiapone<sup>12</sup>, I. Savvidis<sup>20</sup>, G. Tagliente<sup>4</sup>, J.L. Tain<sup>19</sup>, L. Tavora<sup>14</sup>, R. Terlizzi<sup>4</sup>, P. Vaz<sup>14</sup>, A. Ventura<sup>29</sup>, D. Villamarin<sup>6</sup>, M.C. Vincente<sup>10</sup>, V. Vlachoudis<sup>12</sup>, R. Vlastou<sup>27</sup>, F. Voss<sup>18</sup>, S. Walter<sup>18</sup>, C. Weiss<sup>12</sup>, M. Wiesher<sup>17</sup>, and K. Wisshak<sup>18</sup> (n\_TOF Collaboration)

<sup>1</sup>EC-JRC-IRMM, Retieseweg 111, 2440 Geel, Belgium

<sup>2</sup>Universidad de Santiago de Compostela, Santiago de Compostela, Spain

<sup>3</sup>CNRS/IN2P3 – IPN, Orsay, France

<sup>4</sup>INFN, Bari, Italy

<sup>5</sup>CEA, Saclay, Irfu/SPhN, Gif-sur-Yvette, France

<sup>6</sup>CIEMAT, Madrid, Spain

<sup>7</sup>University of Lodz, Lodz, Poland

<sup>8</sup>Atominstytut der Österreichischen Universitäten, Technische Universität Wien, Austria

<sup>9</sup>CNRS/IN2P3 – IPHC, Strasbourg, France

<sup>10</sup>Charles University, Prague, Czech Republic

<sup>11</sup>Universitat Politècnica de Catalunya, Barcelona, Spain

<sup>12</sup>CERN, Geneva, Switzerland

<sup>13</sup>Universidad de Sevilla, Sevilla, Spain

<sup>14</sup>Instituto Superior Técnico/CTN, Universidade de Lisboa, Portugal

<sup>15</sup>LIP-Coimbra, Coimbra, Portugal

<sup>16</sup>Instituto Nazionale di Fisica Nucleare, Bari, Italy

<sup>17</sup>Department of Physics and Astronomy, Uppsala University, Sweden

<sup>18</sup>Karlsruhe Institute of Technology, Institut für Kernphysik, Campus North, Karlsruhe, Germany

<sup>19</sup>Instituto de Física Corpuscular, CSIC-Universidad de Valencia, Spain

<sup>20</sup>Aristotle University of Thessaloniki, Greece

<sup>21</sup>Instituto Nazionale di Fisica Nucleare, Trieste, Italy

<sup>22</sup>Joint Institut for Nuclear Research, Frank Laboratory of Neutron Physics, Dubna, Russia

<sup>23</sup>IPPE, Obninsk, Russia

<sup>24</sup>Instituto Nazionale di Fisica Nucleare, Laboratori Nazionali di Legnaro, Italy

<sup>25</sup>Los Alamos National Laboratory, New Mexico, USA

<sup>26</sup>Tokyo Institute of Technology, Tokyo, Japan

<sup>27</sup>National Technical University of Athens (NTUA), Greece

<sup>28</sup>Dipartimento di Fisica, Università di Bologna, Italy

<sup>29</sup>ENEA, Bologna, Italy

<sup>30</sup>Department of Physics and Astronomy, University of Basel, Switzerland

<sup>a</sup> Corresponding author: carlos.PARADELA-DOBARRO@ec.europa.eu

**Abstract.** The  $^{235}\text{U}$  neutron-induced cross section is widely used as reference cross section for measuring other fission cross sections, but in the resonance region it is not considered as an IAEA standard because of the scarce experimental data covering the full region. In this work, we deal with a new analysis of the experimental data obtained with a detection setup based on parallel plate ionization chambers (PPACs) at the CERN n\_TOF facility in the range from 1 eV to 10 keV. The relative cross section has been normalised to the IAEA value in the region between 7.8 and 11 eV, which is claimed as well-known. Comparison with the ENDF/B-VII evaluation and the IAEA reference file from 100 eV to 10 keV are provided.

## 1 Introduction

The  $^{235}\text{U}$  neutron-induced fission cross-section is of greatest importance for reactor physics, and has been extensively studied since the earliest nuclear research. Hence, it has become one of the main references for neutron-induced measurements, being used in a large number of applications involving neutron dosimetry or monitoring. Nevertheless, it is only considered as a standard at the thermal point and in the fast energy range (150 keV-30 MeV), leaving certain room to improve its knowledge in the resonance region.

On the other hand, different fission cross sections measured at the CERN - n\_TOF facility have been released in the last years, using as reference the  $^{235}\text{U}$  cross section [1,2], or even providing the ratio to it [3]. Moreover, it has been employed to obtain the n\_TOF neutron flux at high energies [4]. However, the  $^{235}\text{U}(n,f)$  cross section data from n\_TOF has been released only for a limited range of the resonance region, that are presently in EXFOR [5]. In this work, we report on an improved release of the fission cross section in the range between 1 eV and 10 keV, where the n\_TOF flux shape is smooth and very well known. These data are compared to the ENDF/B-VII evaluated dataset and to the integral values given by the IAEA reference file.

## 2 Experimental setup

We will focus on the data obtained with the detection setup based on Parallel Plate Avalanche Counters (PPAC) used during the n\_TOF experiment Phase-I, when the detection setup consisted of ten detectors and nine targets interleaved, placed perpendicularly to the neutron beam [1]. The data provided in this work are the sum of the three different measurements taken during the 2003 fission campaign. Between the different measurements, the chamber was removed from the Experimental Area to replace part of the targets. However, the first and the second target in the beam direction,  $^{238}\text{U}$  and  $^{235}\text{U}$ , respectively, were not changed.

The targets were made very thin and the detector layers were minimised, being operated at a very low gas pressure. Furthermore, special attention was devoted to minimise too the amount of material in the experimental area, using thin Kapton windows to separate the chamber gas from the evacuated beam pipe. Altogether, the amount of in-beam scattered neutrons was reduced and, moreover, the upstream position of the  $^{235}\text{U}$  target in the experimental setup minimises any possible attenuation from the in-beam materials.

The low background achieved at the CERN - n\_TOF facility is one of the main characteristics of these experiments. Contrary to other time-of-flight facilities such as WNR in LANL or GELINA at JRC-IRMM, n\_TOF has a very long flight-path with the experimental area placed at around 185 m from the spallation target, which reduces the time-independent neutron background. In addition, the duty factor is very low, in the order of seconds, which eliminates completely the background due to in-beam neutrons from the previous pulses (overlap neutrons) and reduces significantly the contribution from fissions events induced by thermal neutrons backscattered in the surrounding walls.

The use of the same detector configuration and very similar experimental conditions resulted in three data sets which agree within their statistical uncertainties.

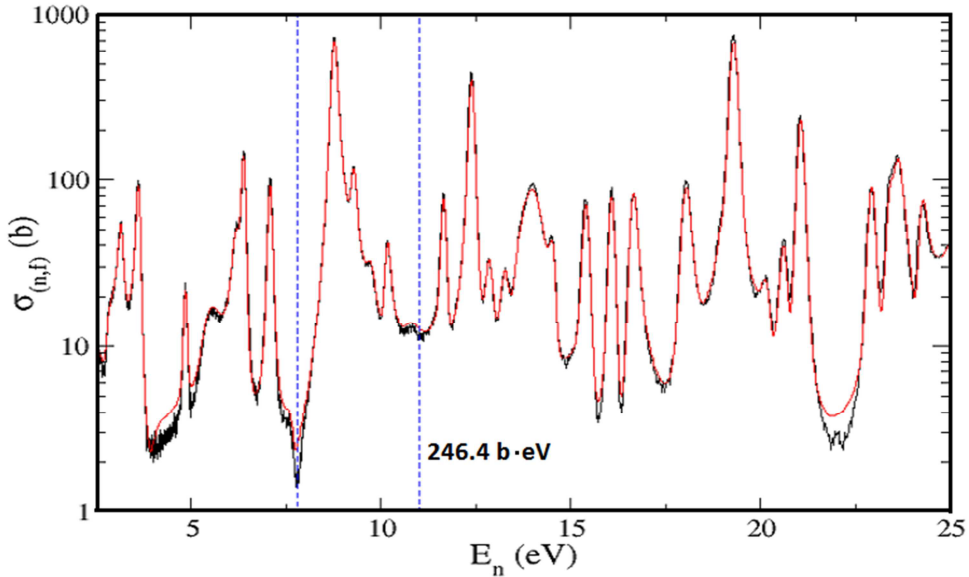


**Figure 1.**  $^{235}\text{U}(n,f)$  cross section in the energy range from 2.5 to 25 eV. The n\_TOF PPACs result (2000 bins per decade) is compared with the ENDF/B-VII evaluation. Vertical lines indicate the IAEA reference interval.

### 3 Data analysis and results

The analysis of the  $^{235}\text{U}(n,f)$  cross section in the low energy region is based on the procedure described in Ref. [1], where the cross sections of  $^{234}\text{U}$  and  $^{237}\text{Np}$  were obtained using  $^{235}\text{U}$  as reference isotope. For this analysis we have included all results taken during the 2003 fission campaign, by directly adding the fission yields obtained in the three data taking periods. Once the final yield is produced, the fission cross section shape is determined by dividing this yield by the official neutron flux provided by measurements with different neutron monitors based on the reference cross sections of  $^6\text{Li}(n,t)$  and  $^{10}\text{B}(n,\alpha)$  during the capture campaign in Phase-I. A comparison between measurements taken with a  $^{10}\text{B}$ -based chamber using both the fission and capture collimators shows that the shape of the neutron flux in the region of interest is conserved below 1% through the collimator change.

In order to provide an accurate normalisation for the obtained fission cross section shape, we have used the well-known 7.8 to 11.0 eV fission resonance integral. With this method, it is neither necessary to know the mass of the  $^{235}\text{U}$  and  $^{10}\text{B}$  deposits nor the efficiency of the detection setup, only assuming that it is constant in the considered energy range. A normalisation value for this integral of  $246.4 \pm 1.2 \text{ b} \cdot \text{eV}$  has been taken from the IAEA standards library [6]. In Figures 1 and 2, the n\_TOF  $^{235}\text{U}(n,f)$  cross section is compared to the current ENDF/B-VII evaluation [7] for two different neutron energy regions. It is worth to mention that the ENDF integral value for the 7.8-11 eV interval ( $241.6 \text{ b} \cdot \text{eV}$ ) differs by 2 % from the IAEA reference value used in this work for the cross section normalisation.

An excellent reproduction of the resonance structure is achieved thanks to our good energy resolution, while the significant statistics allow us to show the different behaviour in the dips. The excellent background conditions led to reduced counts in the dips between resonances (see in Fig. 1). On the other hand, it is worth to note a problem with the energy calibration of the ENDF data above 100 eV. The complete n\_TOF dataset, including uncertainties, will be available in EXFOR.

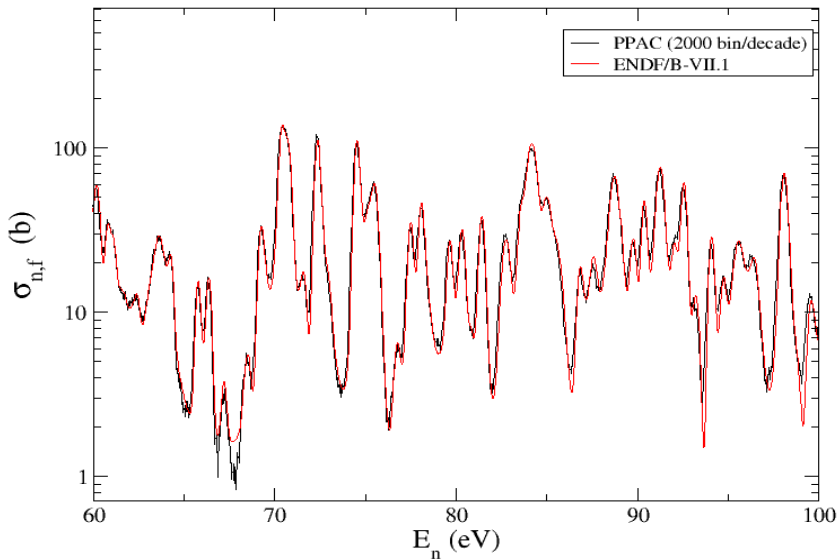


**Figure 2.**  $^{235}\text{U}(n,f)$  cross section in the energy range from 60 to 100 eV.

#### 4 Averaged integral values

In Table 1 the  $n_{\text{TOF}}$  values are compared with those provided in the IAEA reference file, as well as with the ones taken from the ENDF/B-VII data base. All these values are averaged cross-sections (in barn) centred in the same energy intervals as given by IAEA in Ref. [6]. Those from  $n_{\text{TOF}}$  were normalised as previously mentioned but those from ENDF maintain its original normalisation.

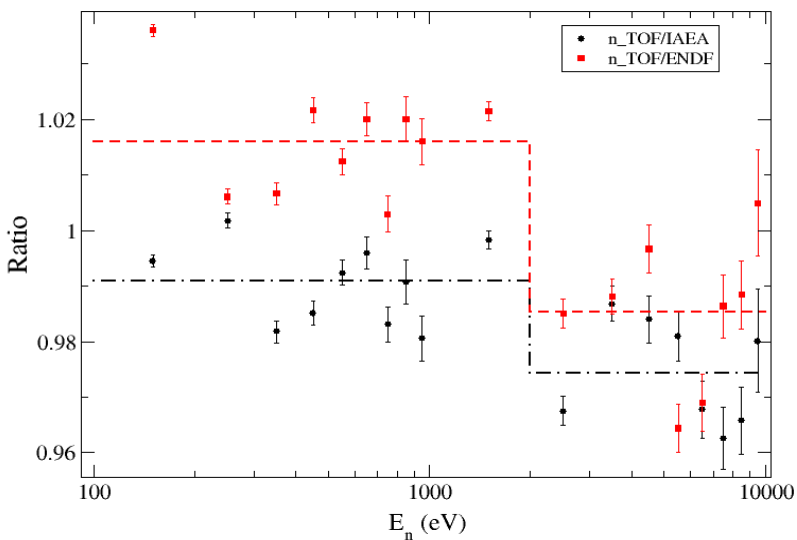


**Figure 3.** Ratios of the  $n_{\text{TOF}}$  data to IAEA reference values (black dots) and to ENDF/B-VII (red squares).

In order to clearly show the existing differences between the IAEA recommended values and those obtained from the ENDF evaluation, we have calculated their ratio with respect to the present results.

These ratios are shown in Fig. 3, centred in the intervals as in Table 1, with error bars corresponding to their statistical uncertainties. The dashed lines represent the average values below and above 2 keV. The abrupt drop in the ratio with the ENDF/B-VII evaluation denotes the influence of different experimental sources above and below 2 keV, corresponding to the transition at around 2.25 keV from the resolved to the unresolved resonance regions in the ENDF evaluation.

On the other hand, an offset appears in Table 1 as a systematic deviation of our dataset from the IAEA one. To some extent this offset could be due to the low background in the  $n_{\text{TOF}}$  experiment. Fig. 4 shows the new ratios after subtracting 0.09 b from every value in the IAEA file (the error bars also include the IAEA reported uncertainties). The ratio distribution along the whole energy range is now extremely flat, its mean value is 0.998, and the spread is compatible with the low statistical uncertainties of the  $n_{\text{TOF}}$  data, endorsing so the goodness of both  $n_{\text{TOF}}$  and IAEA datasets.

**Table 1.** Averaged integral cross-sections (in barn) compared to the IAEA reference file [6] and to ENDF/B-VII. Uncertainties included between brackets refer to the last significant digits.

$E_n$ [eV]	$n_{\text{TOF}}$ [b]	IAEA [b]	ENDF/B-VII [b]
100-200	21.054(22)	21.17(11)	20.321
200-300	20.726(28)	20.69(11)	20.601
300-400	12.891(26)	13.135(72)	12.806
400-500	13.575(30)	13.781(76)	13.288
500-600	15.055(35)	15.174(86)	14.870
600-700	11.463(33)	11.513(65)	11.238
700-800	10.912(35)	11.101(64)	10.880
800-900	8.137(32)	8.213(48)	7.977
900-1000	7.356(30)	7.502(44)	7.240
1000-2000	7.291(12)	7.303(40)	7.138
2000-3000	5.211(14)	5.386(33)	5.290
3000-4000	4.721(15)	4.784(30)	4.778
4000-5000	4.193(16)	4.261(25)	4.207
5000-6000	3.766(17)	3.838(24)	3.905
6000-7000	3.185(17)	3.291(21)	3.287
7000-8000	3.115(18)	3.236(19)	3.158
8000-9000	2.906(18)	3.009(18)	2.940
9000-10000	3.058(29)	3.120(19)	3.043

## 5 Conclusions

A new analysis of the  $^{235}\text{U}(n,f)$  data taken with PPAC detectors at the CERN- $n_{\text{TOF}}$  facility are presented in the energy range 100 eV to 10 keV. The data show extremely low background and very high energy resolution and have been normalised to the IAEA recommendation for the integral value in the range 7.8 to 11.0 eV. Its comparison with the last IAEA reference files and with the present version of the ENDF evaluation leads to the following conclusions:

- There is very good agreement with the shape of the ENDF cross-section in the RRR, while showing a lower background.
- The ENDF integral values, apart from a 2% difference in the normalisation value at 7.8-11.0 eV, show a sharp drop at the transition from the resolved to the unresolved resonance energy regions.

- c) There is very good agreement with the IAEA integral-data set, provided that an offset of 0.09 barn is applied in the whole energy range.

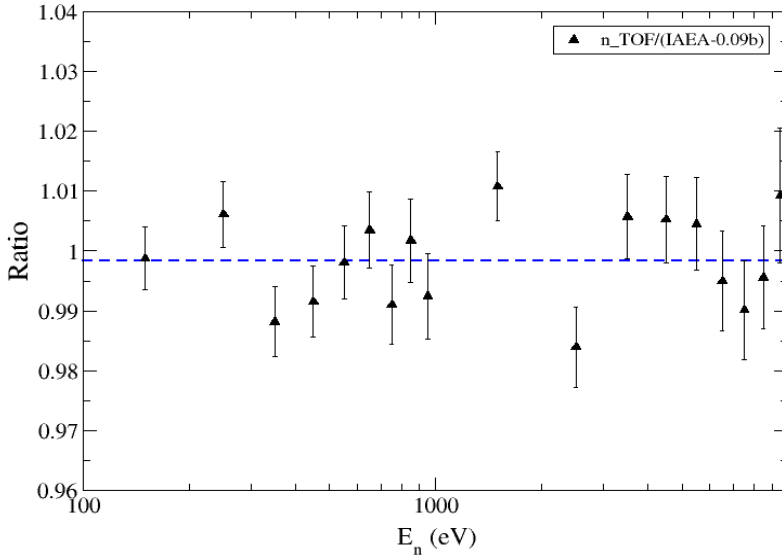


**Figure 4.** New ratio of the  $n_{\text{TOF}}$  data to the IAEA reference values, after applying a 0.09 b offset. The mean value is shown by the blue line.

## References

1. C. Paradela *et al.*, Phys. Rev. C **82**, 034601 (2010)
2. D. Tarrío *et al.*, Phys Rev. C. **83**, 044620 (2011)
3. C. Paradela *et al.*, Phys. Rev. C **91**, 024602 (2015)
4. M. Barbagallo *et al.*, Eur. Phys. J. A (2013) **49**: 12 - 24
5. C. Guerrero *et al.*, Eur. Phys. J. A. (2013) **49**: 27- 42
6. L. Audouin *et al.*, Proc. of Conf. on Nucl. Data for Sci. and Tech., Nice 2007, Vol. 1, p. 421.
7. <https://www-nds.iaea.org/standards/>
8. M.B. Chadwick *et al.*, Nucl. Data Sheets **112**, 2887 (2011)